Proceedings of the Project Review, Geo-Mathematical Imaging Group (Purdue University, West Lafayette IN),
Vol. 1 (2010) pp. 187-200.

RECURSIVE IMAGING WITH MULTIPLY-SCATTERED WAVES USING PARTIAL IMAGE REGULARIZATION: A NORTH SEA CASE STUDY

ALISON E. MALCOLM*, MAARTEN V. DE HOOP†, AND BJØRN URSIN‡

Abstract. As more and more resources are directed toward reverse-time migration an accurate velocity model, including strong reflectors, is necessary to form a good image of the subsurface. This is of particular importance in the vicinity of salt, where singly scattered waves are often not ideal for imaging the salt flanks. This has led to interest in processing doubly scattered waves (also called duplex or prismatic waves) for imaging salt flanks and thus improving the location of salt boundaries in a velocity model. We present a case study of using doubly scattered waves in a two-pass one-way method to image salt flanks in a North Sea data set. By working in the one-way framework we are able to separately construct images with singly, doubly, and triply scattered waves and to use a standard image as the multiple-generating interface, allowing for energy from several reflectors, potentially with poor continuity, to be included.

1. Introduction. In two related papers, Farmer et al. (2006) and Jones et al. (2007), show how so-called prismatic reflections (double-scattered waves) can be included in a reverse-time migration procedure, by including a reflector in the velocity model, to improve the location of salt flanks in a North Sea data set. We use the same data set to demonstrate a recursive, data driven, one-way approach we introduced in Malcolm et al. (2009). There are several advantages to using a such an approach for this imaging problem. The first is that in the recursive approach a standard image is used as the multiple-generating interface, removing the need to pick a reflector and include it in the background velocity model; for this data set this moves the imaged salt flank. (We will use the word 'multiple' here to refer to any wave that has scattered more than once, thus doubly scattered, prismatic, or duplex waves are considered multiples.) In addition, by imaging in a one-way approach we have control of the various wave constituents and their direction of propagation. This allows separate images to be produced from singly, doubly and triply scattered waves; the total image is simply the sum of these contributions. It is then possible to interpret these images separately, and to highlight and remove any artifacts from each image. The use of one-way methods, although limiting somewhat in terms of high-angle accuracy, reduces the computational cost of the procedure.

Doubly-scattered waves, referred to as either duplex waves or prismatic reflections in the literature, have been considered as a source of additional information for some time. In Bell (1991), they are used to explicitly locate a vertical reflector by reducing the traveltime of a doubly scattered wave to that of a primary. The effect of doubly scattered waves on dip moveout algorithms is discussed by Hawkins (1994). Bernitsas et al. (1997) demonstrates the artifacts expected in subsalt imaging from prismatic reflections. In a more modern imaging context, Marmalyevskyy et al. (2005) uses a ray-theoretic approach and an explicitly picked near-horizontal reflector to image a near-vertical reflector with doubly scattered waves; this is adapted and applied to a real data set by Link et al. (2007). The work of Broto and Lailly (2001); Cavalca and Lailly (2005, 2007) also uses ray theory and doubly scattered waves, but in the context of developing an inversion algorithm that allows for regions in which particular events are not recorded or do not exist. This is particularly important for doubly scattered waves as they are rarely recorded throughout the survey extent. Most recently, Marmalyevskyy et al. (2008); Kostyukevych et al. (2009) compute transmission coefficients for doubly scatterd waves to allow their migration in a Kirchoff method for a VSP geometry in fractured media.

Our method for imaging with multiply scattered waves has similarities to the two-pass one-way methods proposed first by Hale et al. (1991) for imaging turning waves, in which the wavefield is first propagated down into the subsurface and stored at depth and then propagated back to the surface in a second pass. More recent discussions of these methods can be found in Xu and Jin (2006) and Zhang et al. (2006). The difference between turning wave imaging and double scatter imaging is in the inclusion of a reflection from the lower boundary. This was done using the multiple forward, single back-scatter method in Jin et al. (2006); Xu and Jin (2007). By contrast, we use a standard image as the multiple-generating reflector, rather than explicitly

*Department of Earth, Atmospheric and Planetary Sciences, Massachusetts Institute of Technology
†Center for Computational and Applied Mathematics and Geo-Mathematical Imaging Group, Purdue University, West Lafayette, IN 47907, USA
‡Department of Petroleum Engineering and Applied Geophysics, Norwegian University of Science and Technology, Trondheim, Norway

including this reflector in the velocity model. The use of an image for the multiple-generating reflector also sets our method apart from the reverse time methods mentioned above (Farmer et al., 2006; Jones et al., 2007), in which the reflector is included in the velocity model. Our method assumes that multiples do not generate artifacts in this single-scatter image, or that they have been removed.

There is no fundamental difference between imaging with doubly and triply scattered waves (multiples). Thus far, however, most imaging with multiply scattered waves has focussed on surface-related multiples as these are the simplest to understand and the closest, in many ways, to singly scattered waves because the multiple-generating reflector is well known (sea surface). Beginning with the work of Reiter et al. (1991) who proposed a method for imaging with water-column multiples in a Kirchhoff scheme and continuing through the recent work of Berkhout and Verschuur (2003, 2004, 2006) in which surface-related multiples are converted into primaries, surface-related multiples have been shown to provide added information in imaging. There are also several discussions for particular acquisitions, such as VSP (Jiang, 2006) and OBC (Muijs et al., 2007) as well as more in depth inversion procedures such as that suggested by Métivier et al. (2009). For the more complicated situation of internal multiples, most studies exploiting these events rely on interferometry to record at depth and subsequently convert internal multiples into primaries (Schuster et al., 2004; Jiang et al., 2005, 2007; Vasconcelos et al., 2007). These methods are somewhat similar to the Berkhout and Verschuur (2006) methods in that they remove one leg of the propagation via cross-correlation. Mittett (2002, 2006) discusses the inclusion of multiples in reverse-time migration with a specific focus on data requirements for multiples to image correctly, without causing artifacts in the image. Youn and Zhou (2001) describe a method, based on finite differences, that allows for the simultaneous imaging of primaries, internal and surface-related multiples that requires detailed velocity information and requires additional computational resources compared to other methods.

As is to be expected, when imaging with the relatively low amplitude multiply scattered waves data sampling becomes more important than for the single-scattering case. There are many different ways of interpolating and filling in data; a relatively recent review of methods can be found in e.g. Stolt (2002). Here, we chose to use a wave packet based method that both fills in missing data and denoises concurrently, through sparsity promoting optimtimization. This method of regularizing data goes back to Daubechies and Teschke (2005), in which iterative thresholding was applied to images in order to simultaneously deblur and denoise them. This method was developed further for the seismic case by Hennenfent and Herrmann (2006), in which they discuss the curvelet transform, introduced in Candès et al. (2006), with particular emphasis on nonuniformly sampled data. More details on the algorithm used here can be found in Andersson et al. (2010).

This paper has three main sections, the first summarizes the imaging with multiples method as well as the regularization method. The second uses synthetic data to illustrate sampling issues when imaging with multiply scattered waves and the third discusses the application of the methods on a data set from the North Sea.

2. Summary of Methods. The procedure for imaging with multiply scattered waves employed here is discussed in detail in Malcolm et al. (2009), here we give a summary of the most important ideas, without discussing the underlying theory. The method builds on previous work in Malcolm and de Hoop (2005) which combines two series approaches, the Generalized Bremmer series (de Hoop, 1996) and the Born series discussed by Weglein et al. (2003).

The basic structure of our technique for imaging with multiply scattered waves is straightforward. The procedure is broken into the following steps, illustrated in Figure 1,

1. Form a standard image, assuming singly scattered waves.
2. Propagate the surface data down into the subsurface (with a one-way method), multiply the wavefield by the image, formed in 1, and store the resulting composite wavefield at each depth (Figure 1(a)).
3. Propagate the composite wavefield up to the surface (Figure 1(b)), forming an image at each depth by applying the imaging condition to the two composite wavefields for internal multiples, and to one composite wavefield and the standard downward continued wavefield for doubly-scattered waves (Figure 1(c)).

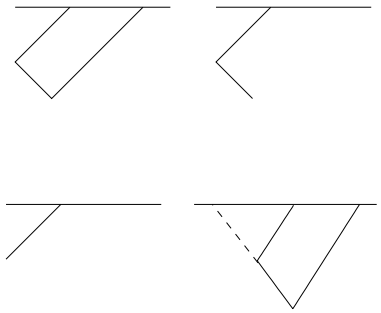

FIG. 1. *The data shown in (a), are first downward continued (here illustrated on the receiver side) and multiplied by the image, at x_1 as in (b), after which the resulting composite wavefield is propagated up to the vertical reflection point at x_2 in (c) where an image is formed by applying the imaging condition to the up-going composite wavefield and the standard downgoing wavefield on the source side. (d) Most of the artifacts, in a double-scatter image are caused by primaries that follow the dashed path, sharing the path of the doubly scattered wave through the first scattering point at x_1; here these are removed with an f-k filter.*

As in reverse-time migration, including multiples requires the specification of a layer (or multiple layers) that generate the multiples (see the discussion in Jones et al. (2007)). This information must be included directly in the velocity model for reverse-time migration, and for the methods of Jin et al. (2006); Xu and Jin (2007). In our method this information is included separately, and is obtained directly from a standard image. This means that only the regions of the image that have significant reflectivity contribute to the generation of multiply-scattered waves, and that it is not necessary to specifically decide all layers that may generate multiples. Of course, it is still possible to exclude multiples from specific layers by simply muting the input image to not include those layers. It is thus not necessary that there be a single coherent reflector, although there must be something that physically reflects the energy toward the salt flank.

Similar to methods discussed by Brown and Guitton (2005), imaging with multiply scattered waves requires the separation of these multiples from primaries. Although a method such as that suggested by Brown & Guitton would likely result in a cleaner image with fewer artifacts, we have found that much simpler procedures are adequate, in particular for doubly scattered waves. For these waves, we observe that most of the artifacts come from the interference of doubly scattered waves with primaries that share part of the path of the doubly scattered waves as illustrated in Figure 1(d). These waves can be removed in a straightforward manner by applying an f-k filter before applying the imaging condition. In the example studied here, we find the best results using a long, smooth filter, that removes waves up to vertical propagation from both the source and receiver-side wavefields.

2.1. ℓ_1 regularization. The basic idea of this regularization method is to first take the curvelet transform of the data, (discussed in Candès et al. (2006)), which results in a decomposition of the data as a function of scale and orientation. Scale gives a measure of the coherency of the wavefield in a particular (spatial) frequency band; coherent structures are at large scales whereas incoherent structures exist over a range of smaller scales. Orientation indicates the direction of the wave packet. We then apply a thresholding and regularization/interpolation in the curvelet domain, similar to that introduced by Daubechies and Teschke (2005) and extended by Hennenfent and Herrmann (2006). In the thresholding procedure, discussed further in Andersson et al. (2010), small scales are removed, to lower the ambient noise level of the signal by removing incoherent events. This is conceptually similar to a low-pass filter although in this case the filter is applied in a domain specifically tailored to wave problems. To regularize the data, the output of the curvelet transform is computed at a denser grid than the input data.

3. Effect of Sampling. To illustrate the importance of sampling in the lateral direction, we begin with a synthetic data set with multiple vertical layers, designed to mimic the structures seen in the real data set discussed in the following section. The velocity model for this data set is shown in Figure 2, along with a standard image made with a shot-record migration using a simple phase-shift propagator, performing the

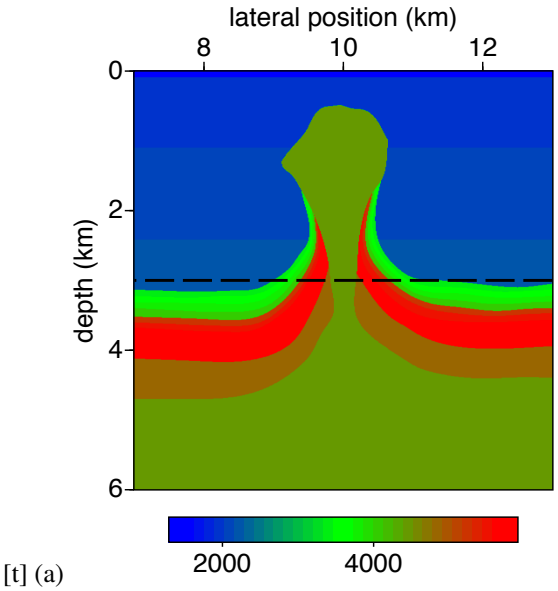

FIG. 2. *(a) Velocity model used to generate the synthetic data set. (b) Image made using data generated in the velocity model in (a).*

phase-shift separately for each occuring velocity in a horizontal slice. This is similar to the PSPI propagator Gazdag and Sguazzero (1984) as well as to the propagators suggested in Ferguson and Margrave (2002). Although the cost is somewhat prohibitive, it is easy to implement and we find this propagator to be sufficiently accurate for this data set. Either this propagator or a simple split-step are used throughout this paper.

Resolving the different vertical layers in this model requires that the image be made on a relatively dense horizontal grid. This does not mean that more data is required than is used to make a standard image, only that the image must be formed on a fine enough grid to appropriately sample the lateral direction. This is illustrated in Figure 3. In this figure two different receiver sampling intervals are used to form the doubly scattered image, both of which are sufficient to see the flank of the salt, but the denser of which (in (b)) results in a clearer, higher resolution image. We also illustrate, by muting every other trace in the data set used to make the more densely sampled image, that more data is not required as the images in (b) and (c)

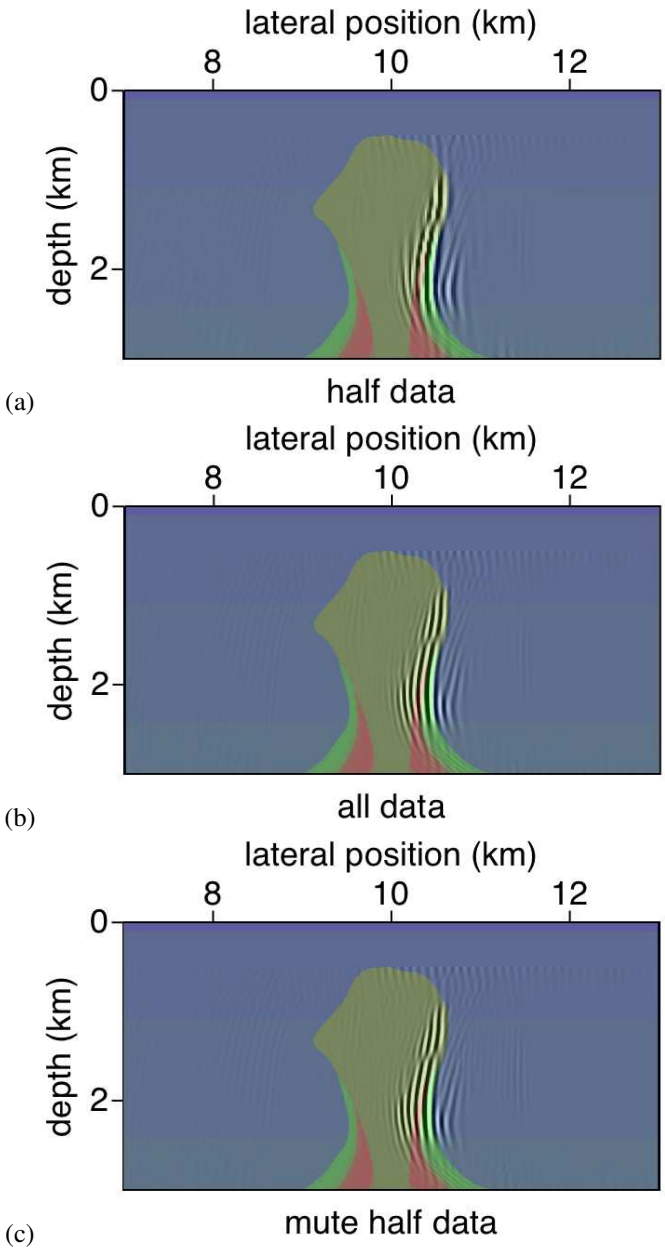

FIG. 3. *The effect of grid size on the final image. (a) Using a receiver spacing of 25 m we get a good image of the vertical salt-flank. (b) Using a receiver spacing of 12.5 m gives the image a higher resolution, although the location and shape of the reflector do not change much. (c) Using the same grid as in (b) for the propagation, but with every second receiver muted (so an effective receiver spacing of 25 m with an actual receiver spacing of 12.5 m) gives nearly the same image as in (b) indicating that the additional data is not required but forming the image on a finer grid improves the image. All of these figures were made using the image shown in Figure 2 muted outside the interval 2.5-3.4 km as the input single-scatter image.*

are nearly equivalent. The image shown in Figure 2(b), muted outside of depth 2.5 to 3.4 km, is used for the input single-scatter image.

4. Application to North Sea Data Set. In this section we explore the possibility of using doubly scattered waves to improve the velocity model near a salt structure that is not well imaged. The data are from a North Sea field; this data set is discussed in more detail in Farmer et al. (2006); Jones et al. (2007), where a

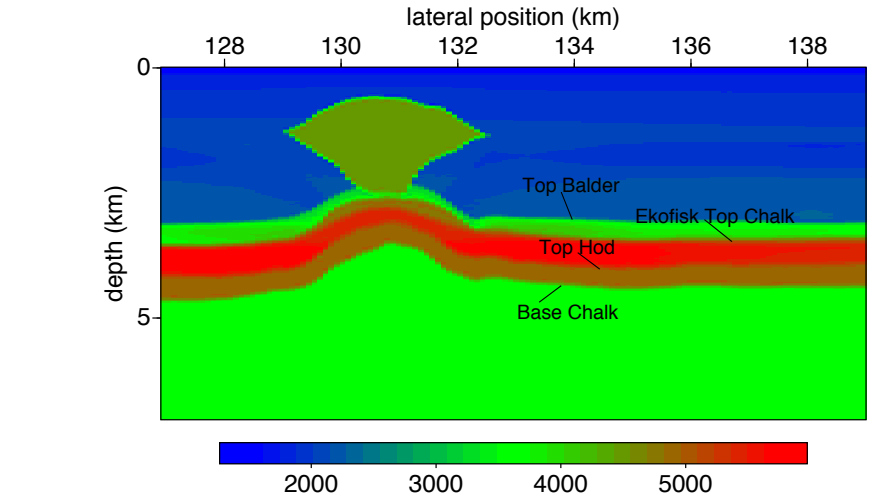

(a)

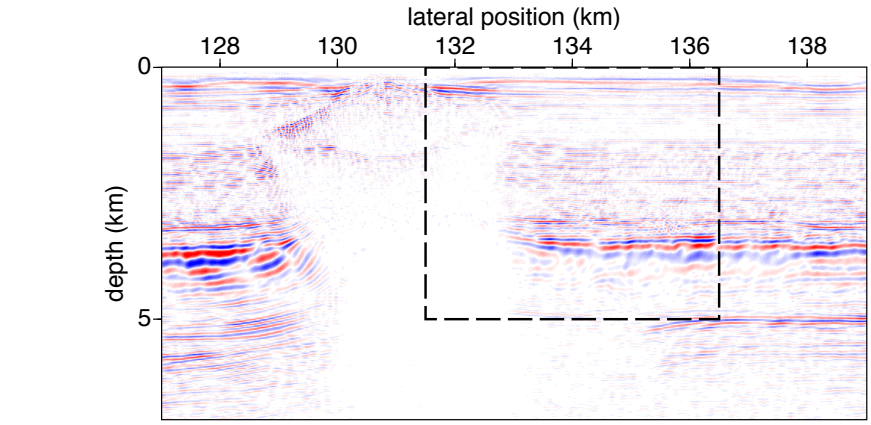

(b)

FIG. 4. *(a) Original velocity model for the real data set. Three different models are used in this case study, the full model, depicted here, the sediment model, which does not include the salt itself and the 1D model which is the first column of this model. (b) Image made with the original data set, including offsets up to 2 km, and the sediment model.*

similar set of procedures are applied in a reverse-time migration framework. What this study adds is, first the removal of the requirement that the salt itself be included in the velocity model, and second the requirement that hard boundaries be included in the velocity model. The first requirement is removed by using only waves that travel outside the salt to image its boundaries. This is similar to the result in Jones et al. (2007) that used reverse time migration to image the salt flanks with duplex waves. The second requirement is removed by separating the smooth background velocity model from the sharp reflectors. By using both an image and a velocity model, we are able to reduce the requirements on the level of detail present in the migration velocity model. The velocity model, estimated through one-way tomography, as discussed in Jones et al. (2007), is shown in Figure 4(a). The images formed here use either this model with the salt removed (sediment velocity model) or a 1D model made by taking the first column of this model. Figure 4(b) shows an image made with all 315 recorded shots on a 2D line extracted from the 3D volume, for each shot 120 offsets are recorded with a minimum offset of 160 m and 25 m spacing, the shot spacing is 50 m. To avoid artifacts caused by waves traveling through the salt, we limit the offsets included in the imaging to 2 km; the image was made with a

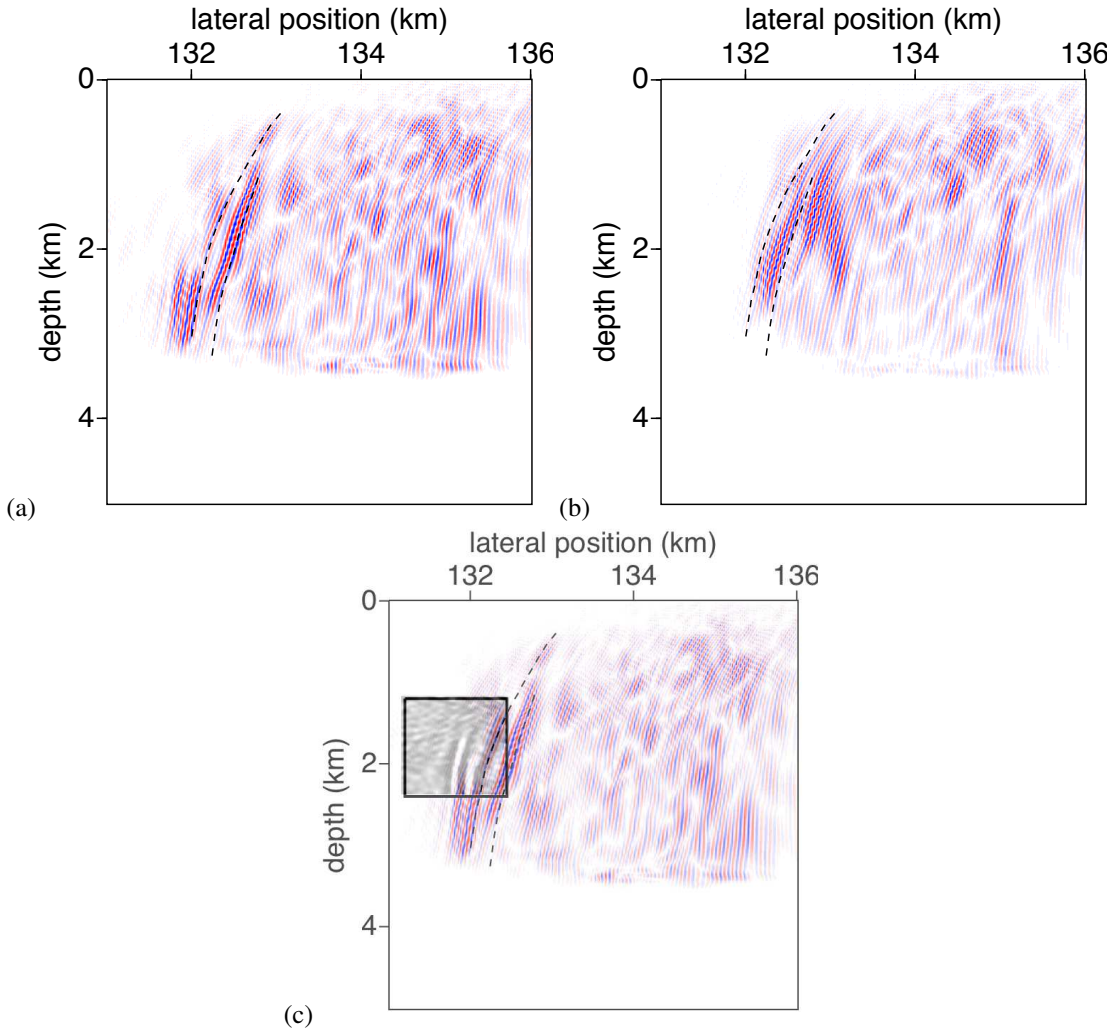

FIG. 5. *This is the double-scatter image made with the original data and (a) the sediment velocity model or (b) the one-dimensional velocity model. (c) Repeats (a) with the image in the box, coming from Jones et al. (2007). Dashed lines mark reflectors picked in Figure 10.*

split-step propagator.

From the migrated image in Figure 4 we see that there is likely a salt dome between approximately 129 and 133 km that is precluding the formation of an image in that region. To improve our ability to image this structure, we first form an image with doubly scattered waves using data recorded to the right of the salt, using 50 shots from 135 to 137.5 km. In forming this image, we restricted the imaging procedure so that the reflection from the multiple-generating interface is only on the receiver side. This is consistent with the recording geometry, as the receivers are all to the right of the source, precluding the recording of source-side multiples. The resulting image is shown in Figure 5, along with a similar image made in a the 1D velocity model. Although these images show a clear salt flank, that is similar to that found in Jones et al. (2007), there is a lot of ringing that detracts from the image quality and the image is relatively low-resolution in the lateral direction.

As a next step, we improve the lateral resolution of the image. Based on the discussion in the previous section, we know that the image of the vertical structure can be greatly improved by simply decreasing the grid size. Although we expect, from that discussion, that simply migrating on a finer grid without increasing the data sampling will improve the image, we decided to first regularize the data because of the ringing and

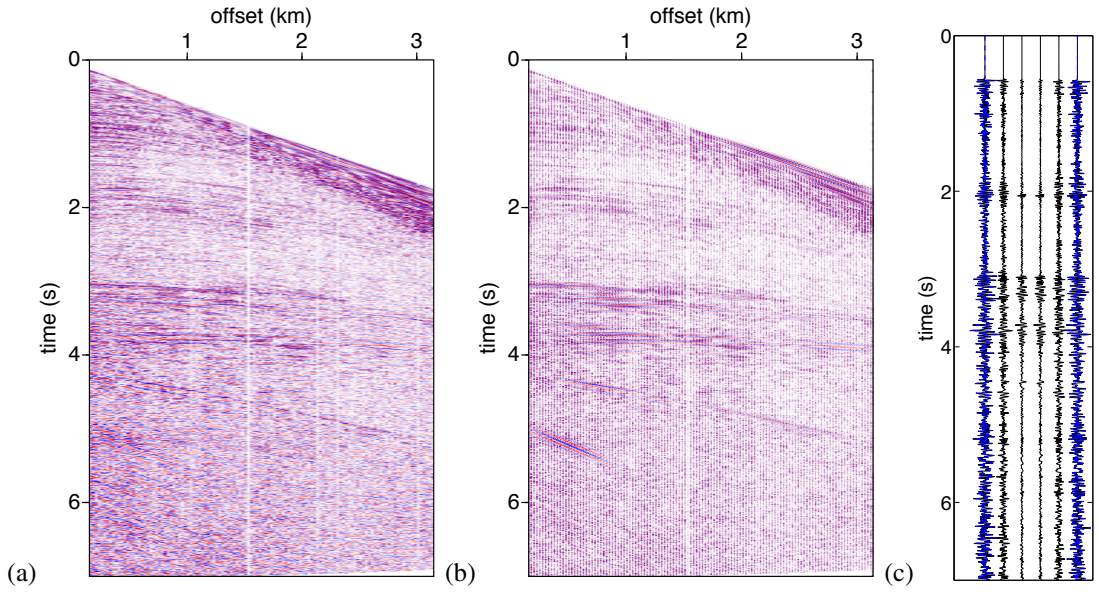

FIG. 6. *(a) Original shot record with shot at 135 km. (b) Shot record regularized and de-noised. (c) Traces from offsets 910 m to 935 m, the black traces are the denoised, regularized traces and the blue lines, which nearly overlay the black, are the original traces at positions where these are available.*

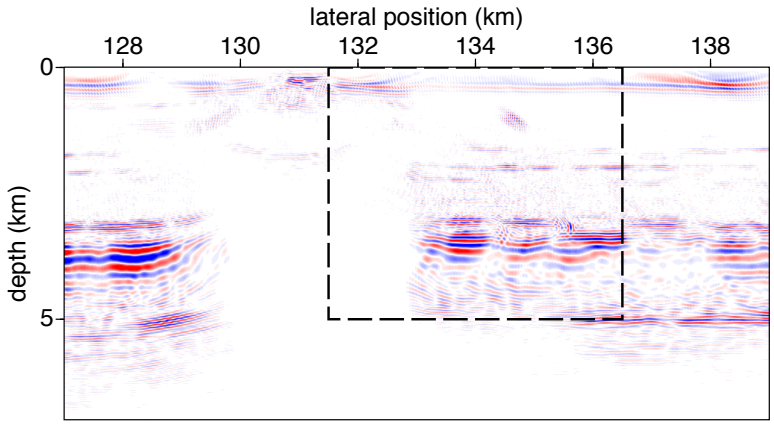

FIG. 7. *Image made with the regularized and denoised data and the sediment velocity model.*

high general noise level in the image. The regularization procedure used is discussed in the methods section, here we used it to denoise and increase by a factor of 5 the receiver sampling (the regularized offset sampling is 5 m). An example of the resulting regularized data is shown in Figure 6, in which we see that the lateral continuity of the reflections is improved. As shown in Figure 6(c) this regularization procedure fills in smaller traces between the original traces because the total energy before and after regularization remains constant, this essentially weights the interpolated traces less in the migration than the original denoised traces. In the image formed from the regularized data, shown in Figure 7, we already see an improvement in the imaging of what may be the base of salt, at approximately 2 km depth and position 131 km. To image the flank of salt or near-vertical chalk layer, we then repeat the double-scatter imaging with three different velocity/single scatter image pairs, the results of which are shown in Figure 8. It is apparent that while the procedure obviously depends on both the input image and the initial velocity model it is relatively robust to small changes in these inputs; obviously drastically changing the multiple-generating reflector does change the positioning of the

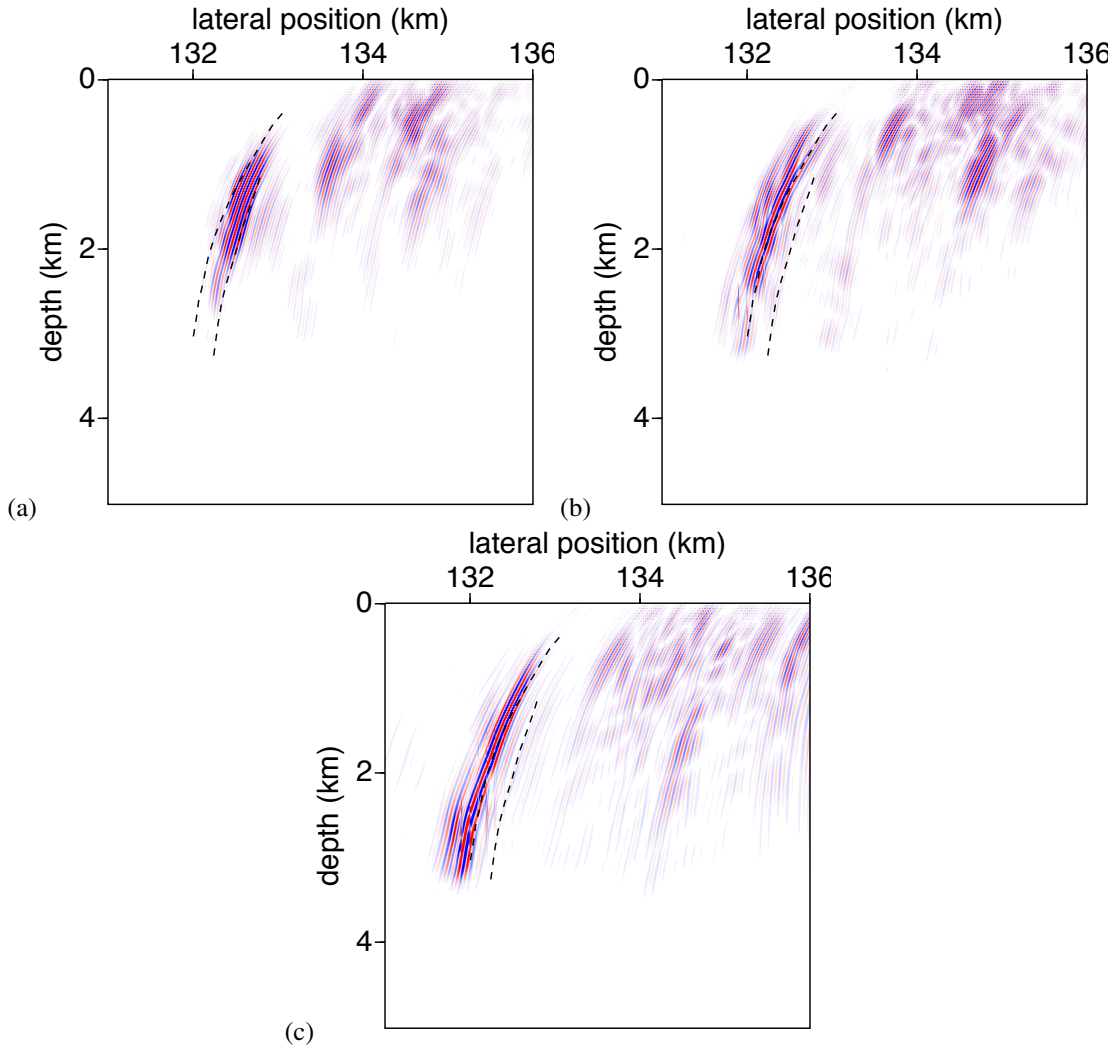

FIG. 8. *(a) Double-scatter image made with the regularized data and the 1D velocity model using a muted version of the image in Figure 7(a) for V_1'. (b) Double-scatter image made with the regularized data and the sediment velocity model,using a muted version of the image in Figure 7(a) for V_1'. (c) Double-scatter image made with the regularized data, the sediment velocity and a flat reflector at a depth of 3390 m image for V_1'. Dashed lines mark the locations of the salt flanks as picked in Figure 10*

salt flank.

The data regularization is able to improve the resolution and also to decrease the ringing in the double-scattered image, but there are still artifacts in the final image. We expect that these come from primaries reflected from the layers with poor lateral continuity between the chalk layer and the water bottom. To remove this ringing we now design a surgical muting procedure to isolate, in the data, the double-scattered energy from the top of the chalk layer. In the current framework, such a procedure is straightforward, we first mute the double-scatter image to isolate the position we think the vertical reflector is in. Second, we isolate the top of the chalk in the regularized image in Figure 7, downsampled back to the original data sampling. It is then straightforward to model the data, using the sources used to form the image, and simply changing the direction of the propagators. This results in a model of the doubly-scattered waves in the data. A surgical mute was then designed by taking data beginning from within a few wavelengths of the modeled doubly scattered waves, this windowing allows for errors in the modeling from mispositioned reflectors and incorrect smooth velocity, but still isolates these events from others in the data, this is shown in Figure 9.

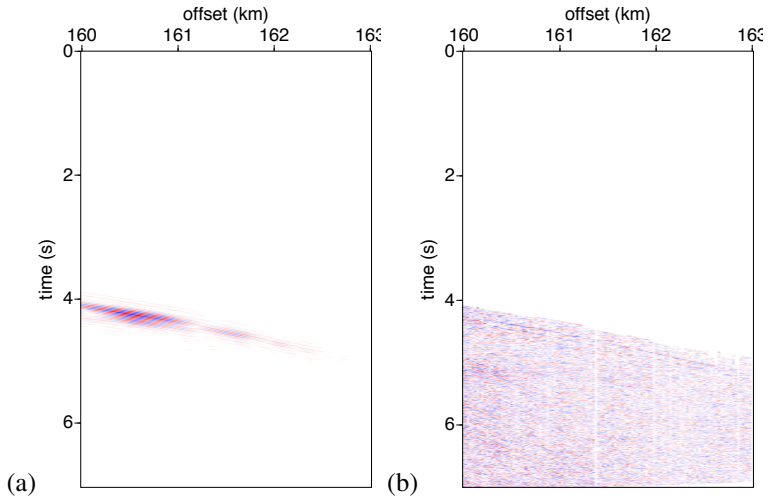

FIG. 9. *(a) Modelled doubly scattered data using the top-chalk reflector and the imaged salt flank as the two reflectors. (b) Original data muted with a mute designed to keep only the doubly scattered data, and later arrivals, based on the modeled data in (a).*

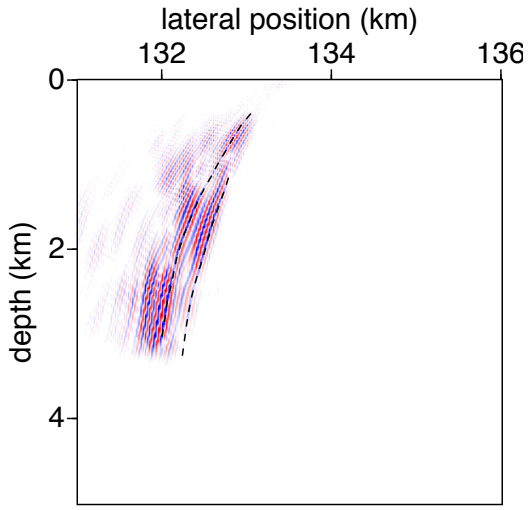

FIG. 10. *Double scattered image made with the surgically muted data, a muted version of the image in Figure 7(a), and the sediment velocity model.*

The resulting muted data set was then used to construct a doubly scattered image shown in Figure 10. As this procedure has almost completely removed the ringing we conclude that the ringing did indeed come from interference of additional events in the data.

We then choose the best image of the salt flanks made with doubly scattered waves to add to these new images to form a final image of the entire region. These final images are shown in Figure 11. Note that the entire imaging procedure was carried out without ever including the salt structure itself in the velocity model.

5. Discussion. Throughout this paper, we have chosen to image only one side of the structures of interest, in part because the data set we obtained had data coverage for only one side of the reflector. Given equivalent source/receiver coverage, of course, one can image either side by reciprocity. Motivated by a typical marine acquisition geometry, we study whether or not equivalent illumination of both flanks of the salt is possible. To this end, we use a simple example in which a single near-vertical reflector is imaged. In

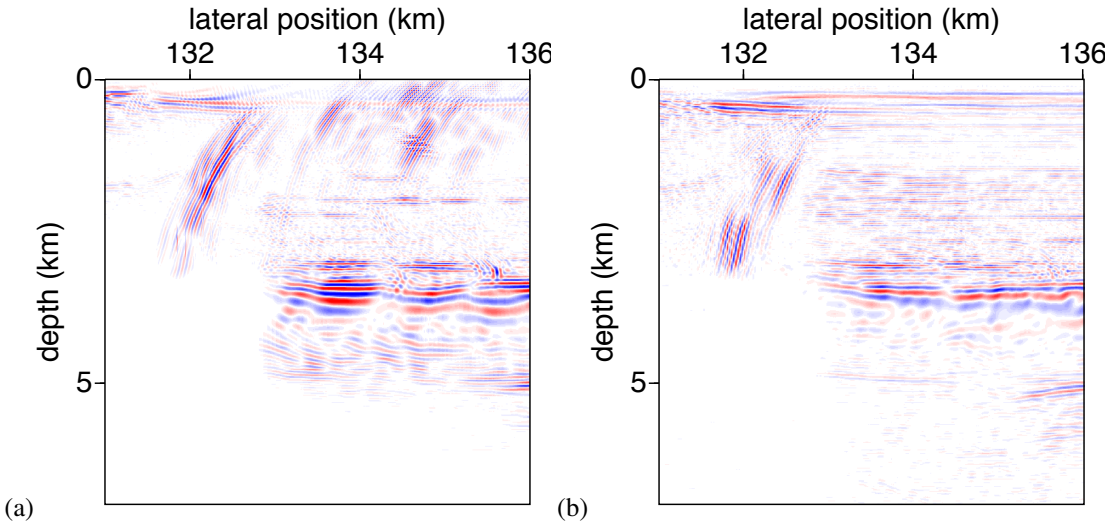

FIG. 11. *(a) Total image including both singly and doubly scattered data for the regularized data set, using the image in Figure 7 muted outside 3.225 to 3.6 km depth as the input single scattered image. The remaining ringing may come from multiply scattered energy within the salt flank. (b) The total image including both singly and doubly scattered waves for the unregularized data set, using the surgically muted data set to make the double scatter image and the image in Figure 4(b) muted outside of 3.225 and 3.6 km as the input single scatter image. Note that both images were made entirely with the sediment velocity model.*

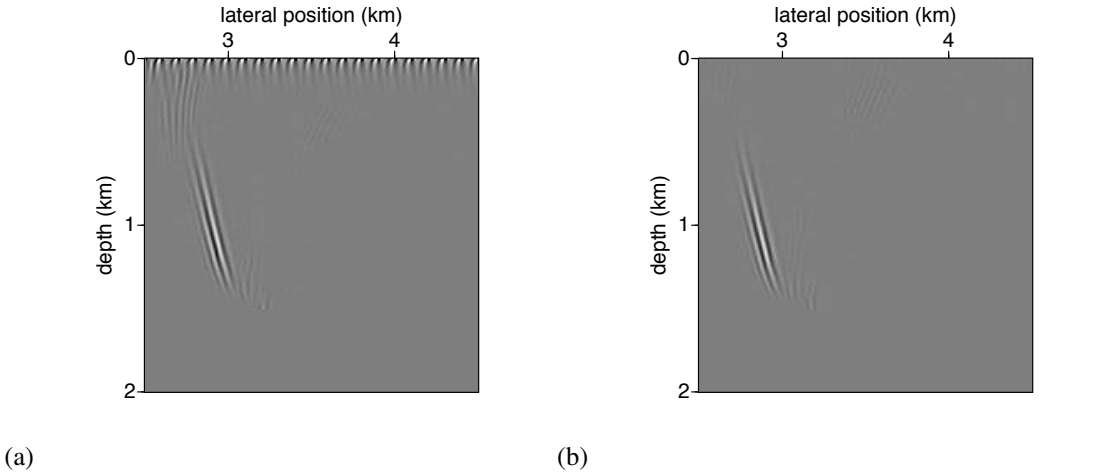

FIG. 12. *(a) Image of a simple curved reflector, made with only 10% of the original shot locations. (b) Same as (a) except that this time only 10% of the receivers were used, with the others muted (so the wave propagation is computed on the same grid).*

this example, sources and receivers are simulated every 10 m, with 250 sources from 2.5 to 5 km and 250 receivers with offsets from 0 to 2.5 km. In Figure 12 we show that there is little difference in the recovered image if the sources or receivers are decimated by a factor of 10, to a sampling of 100 m. This highlights the main difference between towing the streamer toward versus away from the flank to be imaged: the difference in sampling of the wave that reflects from the lower layer. This means that imaging with doubly scattered waves is possible whichever direction the streamer is towed. It is noteworthy, however, that data are required sufficiently far from the flank to allow the recording of doubly scattered waves. Large offsets are less important, the real data set discussed in this paper had offsets up to little more than 3 km, however doubly scattered waves are not likely to be recorded near the salt flank.

Although reverse time migration, or full waveform inversion, are likely to make imaging with one-way

methods obsolete in the near future, there is still a place for one-way methods in the determination of the velocity near complicated structures. Even with the added complication of regularization and two-pass one-way methods, it is still faster to make an image in this way than to use reverse-time methods. There is also the added advantage of the ability to separate images made with singly, doubly and triply scattered waves. These separate images can be used to identify artifacts from cross-talk (as discussed in detail in Brown and Guitton (2005)), and also for an interpreter to assess the likely artifacts in each image separately. By using an image, rather than including the interface directly in the velocity model, discontinuous or poorly imaged structures may still be used to estimate and thus exploit muliply scattered waves.

6. Conclusions. We have shown that two-pass one-way methods are able to image near-vertical structures such as salt flanks on real data, allowing the improvement of the understanding of the shape of these salt structures. Imaging with doubly scattered waves does not require particularly large offsets, but it does require data recorded at some distance from the structure of interest. Sampling is particularly important when imaging vertical structures with small amplitude doubly scattered waves. We have shown that an ℓ_1 regularization procedure contributes significantly to improving images made with both singly and doubly scattered waves.

Acknowledgements. We are grateful to GX Technologies for the data and permission to publish these results. In particular, Ivan Vasconcelos facilitated the data transfer and made several helpful suggestions and Ian Jones helped to identify and extract a relevant 2D data subset, and provided many of his own figures for comparison. In addition, Rune Mittett was particularly helpful in locating some difficult to find references. BU would like to acknowledge financial support from Statoil through VISTA and the Norwegian Research Council through the ROSE project. MVdH was supported in part by the members of the Geo-Mathematical Imaging Group. AM acknowledges funding from the sponsors of the Earth Resources Laboratory and Total.

References.

Andersson, F., M. V. de Hoop, and A. A. Duchkov, 2010, Discrete, almost symmetric wave packets and multi-scale geometrical representation of (seismic) waves: IEEE Transactions on Geoscience and Remote Sensing, in press.

Bell, D. W., 1991, Seismic imaging of steeply dipping geologic interfaces: United States patent.

Berkhout, A. J. and D. J. Verschuur, 2003, Transformation of multiples into primary reflections: SEG Technical Program Expanded Abstracts, **22**, 1925–1928.

———, 2004, Imaging multiple reflections, the concept: SEG Technical Program Expanded Abstracts, **23**, 1273–1276.

———, 2006, Imaging of multiple reflections: Geophysics, **71**, SI209–SI220.

Bernitsas, N., J. Sun, and C. Sicking, 1997, Prism waves – an explanation for curved seismic horizons below the edge of salt bodies: EAGE Expanded Abstracts.

Broto, K. and P. Lailly, 2001, Towards the tomographic inversion of prismatic reflections: SEG Technical Program Expanded Abstracts, **20**, 726–729.

Brown, M. P. and A. Guitton, 2005, Least-squares joint imaging of multiples and primaries: Geophysics, **70**, S79–S89.

Candès, E., L. Demanet, D. Donoho, and L. Ying, 2006, Fast discrete curvelet transforms: Multiscale Model. Simul., **5**, 861–899 (electronic).

Cavalca, M. and P. Lailly, 2005, Prismatic reflections for the delineation of salt bodies: SEG Technical Program Expanded Abstracts, **24**, 2550–2553.

———, 2007, Accounting for the definition domain of the forward map in traveltime tomography – application to the inversion of prismatic reflections: Inverse Problems, **23**, 139–164.

Daubechies, I. and G. Teschke, 2005, Variational image restoration by means of wavelets: simultaneous decomposition, deblurring, and denoising: Appl. Comput. Harmon. Anal., **19**, 1–16.

de Hoop, M. V., 1996, Generalization of the Bremmer coupling series: J. Math. Phys., **37**, 3246–3282.

Farmer, P. A., I. F. Jones, H. Zhou, R. I. Bloor, and M. C. Goodwin, 2006, Application of reverse time migration to complex imaging problems: First Break, **24**, 65–73.

Ferguson, R. J. and G. F. Margrave, 2002, Prestack depth migration by symmetric nonstationary phase shift: Geophysics, **67**, 594–603.

Gazdag, J. and P. Sguazzero, 1984, Migration of seismic data by phase shift plus interpolation: Geophysics, **49**, 124–131.

Hale, D., N. R. Hill, and J. P. Stefani, 1991, Imaging salt with turning seismic waves: SEG Technical Program Expanded Abstracts, **10**, 1171–1174.

Hawkins, K., 1994, The challenge presented by North Sea Central Graben salt domes to all DMO algorithms: First Break, **12**, 327–343.

Hennenfent, G. and F. J. Herrmann, 2006, Seismic denoising with nonuniformly sampled curvelets: Computing in Science and Engineering, **8**, 16–25.

Jiang, Z., 2006, Migration of interbed multiple reflections: SEG Technical Program Expanded Abstracts, **25**, 3501–3505.

Jiang, Z., J. Sheng, J. Yu, G. T. Schuster, and B. E. Hornby, 2007, Migration methods for imaging different-order multiples: Geophysical Prospecting, **55**, 1–19.

Jiang, Z., J. Yu, G. T. Schuster, and B. E. Hornby, 2005, Migration of multiples: The Leading Edge, **24**, 315–318.

Jin, S., S. Xu, and D. Walraven, 2006, One-return wave equation migration: Imaging of duplex waves: SEG Technical Program Expanded Abstracts, **25**, 2338–2342.

Jones, I. F., M. C. Goodwin, I. D. Berranger, H. Zhou, and P. A. Farmer, 2007, Application of anisotropic 3D reverse time migration to complex North Sea imaging: SEG Technical Program Expanded Abstracts, **26**, 2140–2144.

Kostyukevych, A., N. Marmalevskyi, Y. Roganov, and V. Roganov, 2009, Analysis of azimuthally-dependent transmission coefficients of converted PS-waves for duplex migration on transmitted waves: SEG Technical Program Expanded Abstracts, **28**, 1257–1261.

Link, B., N. Marmalevskyi, Y. Roganov, A. Kostyukevych, and Z. Gornyak, 2007, Direct imaging of subtle, zero-throw vertical faulting — a 3D real-data example: SEG Technical Program Expanded Abstracts, **26**, 2359–2363.

Malcolm, A., B. Ursin, and M. de Hoop, 2009, Seismic imaging and illumination with internal multiples: Geophysical Journal International, **176**, 847–864.

Malcolm, A. E. and M. V. de Hoop, 2005, A method for inverse scattering based on the generalized Bremmer coupling series: Inverse Problems, **21**, 1137–1167.

Marmalyevskyy, N., Y. Roganov, Z. Gornyak, A. Kostyukevych, and V. Mershchiy, 2005, Migration of duplex waves: SEG Technical Program Expanded Abstracts, **24**, 2025–2028.

Marmalyevskyy, N., Y. Roganov, A. Kostyukevych, and V. Roganov, 2008, Duplex wave migration and interferometry for imaging onshore data without angle limitations: EAGE Expanded Abstracts.

Métivier, L., F. Delprat-Jannaud, L. Halpern, and P. Lailly, 2009, 2D nonlinear inversion of walkaway data: SEG Technical Program Expanded Abstracts, **28**, 2342–2346.

Mittett, R., 2002, Multiple suppression by prestack reverse time migration: A nail in the coffin: EAGE Expanded abstracts.

———, 2006, The behaviour of multiples in reverse-time migration schemes: EAGE Expanded abstracts.

Muijs, R., J. O. A. Robertsson, and K. Holliger, 2007, Prestack depth migration of primary and surface-related multiple reflections: Part I — Imaging: Geophysics, **72**, S59–S69.

Reiter, E. C., M. N. Toksöz, T. H. Keho, and G. M. Purdy, 1991, Imaging with deep-water multiples: Geophysics, **56**, 1081–1086.

Schuster, G. T., J. Yu, J. Sheng, and J. Rickett, 2004, Interferometric/daylight seismic imaging: Geophysical Journal International, **157**, 838–852.

Stolt, R., 2002, Seismic data mapping and reconstruction: Geophysics, **67**, 890–908.

Vasconcelos, I., R. Snieder, and B. Hornby, 2007, Target-oriented interferometry — Imaging with internal multiples from subsalt VSP data: SEG Technical Program Expanded Abstracts, **26**, 3069–3073.

Weglein, A., F. B. Araújo, P. M. Carvalho, R. H. Stolt, K. H. Matson, R. T. Coates, D. Corrigan, D. J. Foster, S. A. Shaw, and H. Zhang, 2003, Inverse scattering series and seismic exploration: Inverse Problems, **19**, R27–R83.

Xu, S. and S. Jin, 2006, Wave equation migration of turning waves: SEG Technical Program Expanded Abstracts, **25**, 2328.

———, 2007, An orthogonal one-return wave-equation migration: SEG Technical Program Expanded Abstracts, **26**, 2325–2329.

Youn, O. K. and H. Zhou, 2001, Depth imaging with multiples: Geophysics, **66**, 246–255.

Zhang, Y., S. Xu, and G. Zhang, 2006, Imaging complex salt bodies with turning-wave one-way wave equation: SEG Technical Program Expanded Abstracts, **25**, 2323.